Low Silica MCM-41 Composites and Mesoporous Solids

M. T. Janicke,[†,||] C. C. Landry,[‡,§] S. C. Christiansen,[†] S. Birtalan,[‡] G. D. Stucky,[‡] and B. F. Chmelka*[,†]

Department of Chemical Engineering and Departments of Chemistry and Materials, University of California, Santa Barbara, California 93106

Received December 21, 1998. Revised Manuscript Received February 19, 1999

Aluminosilicate MCM-41 mesophase solids have been prepared under alkaline conditions with high degrees of mesoscopic order and silicon-to-aluminum molar ratios approaching unity. One- and two-dimensional solid-state NMR techniques, in conjunction with elemental analyses, infrared spectroscopy, and powder X-ray diffraction (XRD), establish that high concentrations of aluminum have been incorporated into the aluminosilicate MCM-41 frameworks, with retention of mesoscopic order. Hexagonal low silica MCM-41 has been prepared with a bulk molar Si/Al ratio as low as 1.3, while retaining a minimum of three indexable *p*6*mm* reflections in the XRD pattern prior to calcination. Following calcination to remove the structure-directing surfactant molecules, the hexagonal MCM-41 structures are preserved. The decreased thermal stabilities and dealumination of the materials with higher aluminum contents have been studied using 2D ^{27}Al{^{1}H} heteronuclear correlation NMR and ^{27}Al MAS intensity calibration techniques to examine surface structures and quantify Al species present before and after calcination.

1. Introduction

Since the discovery of the M41S family of mesoporous molecular sieves with tailorable pore sizes ranging from 2.0 to 10.0 nm,[1,2] a great deal of interest has been focused on increasing the acidity of the surfactant-organized aluminosilicate frameworks.[1−9] With surface areas often over 1000 m^2/g and well-defined pore sizes that are substantially larger than in zeolites (typically <1 nm), these materials show promise for applications as high pore volume catalysts or adsorbents. However, unlike crystalline zeolitic systems, diffraction and solid-state nuclear magnetic resonance (NMR) spectroscopy investigations have shown the inorganic oxide walls of M41S solids to generally be disordered at the molecular level. Reactivities reported for mesoporous aluminosilicate M41S catalysts have been consistent with such local structural disorder, being similar to those of commercially available amorphous aluminas and aluminosilicates.[10]

Two potential avenues for improving the reaction properties of M41S mesoporous materials center on increasing the concentration of aluminum atoms in the aluminosilicate framework or altering the local coordination of these framework aluminum sites. Such adjustments are anticipated to have a direct effect on the concentration and charge density of exchangeable cations present. The cations are required to compensate the negative framework charges introduced by the incorporation of tetrahedrally coordinated trivalent aluminum atoms into the siliceous walls. Such cations are usually principal interaction sites for guest molecules that diffuse, adsorb, and react in the porous channels. While control of the local aluminum structure and ordering in M41S materials remains a challenging goal, more effort has been directed toward increasing the aluminum content of the mesopore frameworks. Such framework aluminum species are generally tetrahedrally coordinated to oxygen atoms that form covalent bridges to neighboring silica tetrahedra. This is opposed to undesirable dense aluminum oxide or oxy−hydroxide particles, which tend to be comprised of octahedrally coordinated aluminum species that may be occluded within the mesopores or exist in separate bulk phases. Postsynthesis modifications of porous alumino-

* To whom correspondence should be addressed.
† Department of Chemical Engineering.
‡ Departments of Chemistry and Materials.
|| Present address: Max-Planck-Institut für Kohlenforschung, 45470 Mülheim an der Ruhr, Germany.
§ Present address: Department of Chemistry, University of Vermont, Burlington, VT 05405.

(1) Degnan, T. F.; Johnson, I. D.; Keville, K. M. U.S. Patent No. 5,156,828, 1992.
(2) Kresge, C. T.; Leonowicz, M. E.; Roth, W. J.; Vartuli, J. C.; Beck, J. S. *Nature (London)* **1992**, *359*, 710−712. Beck, J. S.; Vartuli, J. C.; Roth, W. J.; Leonowicz, M. E.; Kresge, C. T.; Schmitt, K. D.; Chu, C. T.-W.; Olson, D. H.; Sheppard, E. W.; McCullen, S. B.; Higgins, J. B.; Schlenker, J. L. *J. Am. Chem. Soc.* **1992**, *114*, 10834−10843.
(3) Kolodziejski, W.; Corma, A.; Navarro, M.-T.; Pérez-Pariente, J. *Solid State Nucl. Magn. Reson.* **1993**, *2*, 253−259.
(4) Chen, C.-Y.; Li, H.-X.; Davis, M. E. *Microporous Mater.* **1993**, *2*, 17−26. Chen, C.-Y.; Burkett, S. L.; Li, H.-X.; Davis, M. E. *Microporous Mater.* **1993**, *2*, 27−34.
(5) Luan, Z.; Cheng, C.-F.; Zhou, W.; Klinowski, J. *J. Phys. Chem.* **1995**, *99*, 1018−1024. Luan, Z.; Cheng, C.-F.; He, H.; Klinowski, J. *J. Phys. Chem.* **1995**, *99*, 10590−10593.
(6) Reddy, K. M.; Song, C. *Catal. Lett.* **1996**, *36*, 103−109.
(7) Janicke, M.; Kumar, D.; Stucky, G. D.; Chmelka, B. F. *Stud. Surf. Sci. Catal.* **1994**, *84*, 243−250.
(8) Luan, Z. H.; He, H.; Zhou, W.; Cheng, C.-F.; Klinowski, J. *J. Chem. Soc., Faraday Trans.* **1995**, *91*, 2955.
(9) Kloetstra, K. R.; Zandbergen, H. W.; van Bekkum, H. *Catal. Lett.* **1995**, *33*, 157−163.
(10) Corma, A.; Martínez, A.; Martínez-Soria, V.; Montón, J. B. *J. Catal.* **1995**, *153*, 25−31. Armengol, E.; Cano, M. L.; Corma, A.; García, H.; Navarro, M. T. *J. Chem. Soc., Chem. Commun.* **1995**, *5*, 519−520. Climent, M. J.; Corma, A.; Iborra, S.; Navarro, M. C.; Primo, J. *J. Catal.* **1996**, *161*, 783−789.

10.1021/cm981135v CCC: $18.00
Published on Web 04/24/1999

silicates by calcination and ion exchange are known to promote the appearance of such extra-framework species,[11,12] which may affect the adsorption or catalytic properties of M41S materials.

Previous attempts to synthesize ordered mesoporous aluminosilicates with aluminum contents high enough to increase appreciably their reactivities have been partially successful, but have tended to yield materials with reduced degrees of mesoscopic organization. For example, earlier studies have reported diminished ordering of MCM-41 mesostructures when molar silicon-to-aluminum (Si/Al) ratios of 13 or lower have been used in the synthesis gels.[5,8] X-ray diffraction patterns of such materials often show only a single low-angle reflection, from which detailed conclusions regarding the structure cannot be made. In addition, samples with high aluminum concentrations (*e.g.*, less than Si/Al $\approx$ 13) often show the appearance of six-coordinate alumina in solid-state ^{27}Al NMR spectra, which is usually considered to represent undesirable extra-framework species.[3−6] It has been observed that crystalline zeolite aluminosilicates generally adhere to Lowenstein's rule,[13,14] which stipulates the avoidance of Al−O−Al framework moieties, leading to a maximum molar aluminum content of Si/Al = 1 for perfectly alternating silica and alumina tetrahedra. Accordingly, it is expected that the possibility exists for preparing MCM-41 frameworks with molar Si/Al ratios that approach unity without formation of extra-framework alumina species. Here, we describe synthesis and characterization methods for increasing the concentration of aluminum incorporated into MCM-41 frameworks, with preservation of the materials' mesostructural integrity.

2. Experimental Section

2.1. Syntheses. Previous investigations here indicated that aluminum sources yielding four-coordinate Al species in solution have a favorable influence on the preparation of M41S materials containing tetrahedrally coordinated aluminum atoms.[1,4−7] Aluminum salts, including sodium aluminate and $Al_2(SO_4)_3$, or aluminum alkoxides have been used in these studies to incorporate limited amounts of Al into aluminosilicate M41S frameworks. On the basis of similar solution behaviors under alkaline conditions, a variety of other salt species, such as $AlCl_3$ and $Al(NO_3)_3$, are expected to be similarly suitable. These species hydrolyze rapidly in alkaline solutions to provide monomeric $Al(OH)_4^-$ and $Al(OH)_3$ species that are stable at low concentrations against self-polymerization over the pH range 8−13 under ambient conditions.[15−17] (Under typical reagent storage conditions, however, these hygroscopic species can react readily with water to yield undesirable alumina or boehmite products.) In the presence of hydrolyzed silicate anions at high pH, monomeric aluminum species in solution are known to co-polymerize preferentially with the silicate anions to form aluminosilicate networks;[17] formation of Al−O−Si moieties is favored to a significant extent over Al−O−Al linkages, as reflected by numerous experimental studies (particularly ^{27}Al and ^{29}Si NMR measurements)[18] and theoretical investigations.[19]

Table 1. Elemental Analyses and X-ray Diffraction Results for Low Silica Aluminosilicate MCM-41 Materials[a]

	Si/Al molar ratio (±0.3%)			d_{hkl} spacing (±1 Å)		
sample	gel	as-synthesized	calcined	*hkl*	as-synthesized	calcined
MCM-41a	8.0	4.6	5.0	100	45.5	39.4
MCM-41b	4.0	2.9	2.9	100	41.6	32.5
MCM-41c	1.0	1.3	1.1	100	47.7	37.9
MCM-41d	0.5	1.3	1.0	100	47.7	37.1

[a] The d_{hkl} spacings correspond to the most intense reflection measured before and after calcination of the as-synthesized products.

In this study, aluminum isopropoxide, $Al(O^iPr)_3$, was used as the aluminum source in preparations of aluminosilicate MCM-41 containing high concentrations of aluminum. As a crystalline solid, aluminum isopropoxide is a tetramer with both four- and six-coordinate Al atoms,[20,21] which hydrolyzes slowly under standard storage conditions but converts rapidly to monomeric $Al(OH)_4^-$ species upon hydrolysis in highly alkaline solutions.[16,22] Thus, under the high pH conditions employed here, aluminum isopropoxide yields soluble tetrahedrally coordinated Al precursor species, which favor incorporation of tetrahedral Al into MCM-41 framework sites.

Aluminosilicate MCM-41 materials were synthesized at room-temperature using aluminum isopropoxide ($Al(O^iPr)_3$, Aldrich), sodium hydroxide (NaOH, Fisher), cetyltrimethylammonium bromide (CTAB, Aldrich), and tetraethoxysilane (TEOS, Fluka). For the sample synthesized with a molar Si/Al ratio of 8 in the gel, MCM-41a (see Table 1), the preparation was carried out as described previously with a molar gel composition 1.00 $Al(O^iPr)_3$:847 H_2O:4.32 NaOH:0.95 CTAB:8.00 SiO_2.[23] For samples with molar Si/Al ratios in the synthesis gels less than or equal to 4, the gel compositions were adjusted slightly to accommodate the increased aluminum isopropoxide in the syntheses. The molar gel compositions were 1.00 $Al(O^iPr)_3$:1255 H_2O:4.32 NaOH:2.13 CTAB:x SiO_2, where x = 4.0, 1.0, and 0.5 for samples MCM-41b, MCM-41c, and MCM-41d, respectively. In addition to increased amounts of water and CTAB in the gel, concentrated HBr (Fisher) was added to the synthesis mixture to decrease the pH and thereby promote co-polymerization of the hydrolyzed silica and alumina species.[16] A typical synthesis procedure for these high-Al-content materials (MCM-41b) is as follows: 0.472 g of $Al(O^iPr)_3$ was mixed with 58.3 g of deionized water and 5.00 g of 2 M NaOH and stirred for 1 h. Then 1.80 g of CTAB were added to the resulting clear solution and heated slightly to dissolve the surfactant. After that, 1.93 g of TEOS were combined with this solution, and the gel was continuously stirred for 16 h at room-temperature. Then, 2 h after the addition of the TEOS, concentrated HBr was delivered dropwise to the reaction mixture to decrease the gel pH to 12. After 4 h more, additional HBr was added to the gel to decrease the pH to 11. The synthesis was complete after 16 h total of

(11) Brunner, E.; Ernst, H.; Freude, D.; Fröhlich, T.; Hunger, M.; Pfeiffer, H. *Zeolites: Facts, Figures, Future*; Jacobs, P. A., van Santen, R. A., Eds.; Elsevier Science Publishers B. V.: Amsterdam, 1989.
(12) Garralón, G.; Corma, A.; Fornés, V. *Zeolites* **1989**, *9*, 84−86.
(13) Engelhardt, G.; Michel, D. *High-Resolution Solid State NMR of Silicates and Zeolites*; John Wiley & Sons: New York, 1987.
(14) Breck, D. W. *Zeolite Molecular Sieves: Structure, Chemistry, and Use*; R. E. Krieger Publishing Co.: Malabar, FL, 1984.
(15) Eremin, N. I.; Volokov, Y. A.; Mironov, V. E. *Russ. Chem. Rev.* **1974**, *43*, 92.
(16) Baes, C. F.; Mesmer, R. E. *The Hydrolysis of Cations*; Wiley: New York, 1986.
(17) Swaddle, T. W.; Salerno, J.; Tregloan, P. A. *Chem. Soc. Rev.* **1994**, *23*, 319−325.
(18) McCormick, A. V.; Bell, A. T.; Radke, C. J. *J. Phys. Chem.* **1989**, *93*, 1733−1737. McCormick, A. V.; Bell, A. T.; Radke, C. J. *J. Phys. Chem.* **1989**, *93*, 1741−1744. Mortlock, R. F.; Bell, A. T.; Radke, C. J. *J. Phys. Chem.* **1991**, *95*, 7847−7851.
(19) Schröeder, K.-P.; Sauer, J. *J. Phys. Chem.* **1993**, *97*, 6579−6581.
(20) Akitt, J. W.; Duncan, R. H. *J. Magn. Reson.* **1974**, *15*, 162−165.
(21) Turova, N. Y.; Kozunov, V. A.; Yanovskii, A. I.; Bokii, N. G.; Struchkov, Y. T.; Tarnopolskii, B. L. *J. Inorg. Nucl. Chem.* **1979**, *41*, 5−11.
(22) Jolivet, J. P. Personal communication.
(23) Janicke, M. T.; Landry, C. C.; Christiansen, S. C.; Kumar, D.; Stucky, G. D.; Chmelka, B. F. *J. Am. Chem. Soc.* **1998**, *120*, 6940−6951.

stirring, and the product was subsequently filtered and washed with deionized water.

A careful calcination procedure was followed to remove the surfactant species and thereby yield mesoporous materials.[23] To ensure complete removal of extraneous charge-balancing cations, to provide a proton source for introducing subsequent Brønsted acidity, and to verify Al incorporation in the final product using two-dimensional NMR, the MCM-41d calcined sample was ion-exchanged with NH_4^+ cations as described previously.[23]

2.2. Characterization. The as-synthesized and calcined low silica MCM-41 products were characterized by elemental analysis, powder X-ray diffraction, ^{27}Al and ^{29}Si magic-angle spinning NMR spectroscopy, BET N_2 isotherm analysis, and infrared (IR) spectroscopy. Bulk Si/Al ratios were determined based on elemental analyses of the aluminosilicate samples by Galbraith Laboratories (Knoxville, TN).

X-ray powder diffraction (XRD) data were acquired on a Scintag PAD X diffractometer using Cu Kα radiation and a liquid-nitrogen-cooled germanium solid-state detector. Typically, the data were collected from 1.5 to 10.5° (2θ) with a resolution of 0.02° and a count time of 1.6 s at each point.

Nitrogen adsorption isotherms for BET surface area and pore size distribution measurements were conducted on the calcined aluminosilicate MCM-41 materials using a Micromeritics ASAP 2000 Micropore Analysis System. Before the analysis, 50−100 mg of sample was dehydrated under vacuum at 150 °C for 12 h. During the course of the experiments, the system was allowed to equilibrate for 15 s at each pressure prior to recording the adsorbed or desorbed volume of nitrogen.

Photoacoustic infrared spectra were collected with a Nicolet 850 IR spectrometer and a photoacoustic cell, MTEC Model 300. For the experiments, calcined mesoporous materials were dehydrated in the IR cell at 130 °C and kept in a helium atmosphere. For each sample, 128 IR spectra were added to achieve acceptable signal-to-noise levels.

Solid-state NMR experiments were performed on a Chemagnetics CMX-500 spectrometer using a wide-bore superconducting 11.7-T magnet from Magnex Scientific, Inc. Magic-angle spinning (MAS) NMR experiments were conducted using a Chemagnetics MAS probehead with 7.5-mm zirconia rotors. ^1H and ^{29}Si chemical shifts were referenced to tetramethylsilane, and the solid-state ^{27}Al NMR signals (each a combination of separate chemical shift and field-dependent second-order quadrupolar shift components) have been referenced to a dilute solution of aqueous $Al(NO_3)_3$. Experimental conditions for the individual NMR experiments are presented in their respective figure captions.

An important issue is whether aluminum atoms are retained in the framework after calcination and, if not, whether all of the aluminum is accounted for by the integrated areas of the ^{27}Al NMR peaks that remain. To monitor the signals in the ^{27}Al MAS NMR spectra quantitatively, an internal standard of aluminum nitride of known mass was placed in the MAS rotor with each sample. AlN was chosen for this study, as opposed to single-crystal sapphire,[24] because the isotropic peak of the ^{27}AlN species does not overlap with the MCM-41 aluminum oxide peaks. Two equal amounts (*ca.* 200 mg) of each as-synthesized aluminosilicate MCM-41 material were obtained; after one of the allotments was calcined, ^{27}Al MAS experiments were performed separately on the as-synthesized and calcined samples. Use of the same AlN standard for each experiment allowed the single-pulse ^{27}Al MAS spectra to be calibrated for an accurate comparison of signal intensities from the MCM-41 samples after different treatments. This permitted a quantitative assessment of ^{27}Al signal loss that appears to be attributable to the formation of so-called "NMR invisible" ^{27}Al following calcination.

3. Results and Discussion

3.1. Elemental Analysis. Aluminosilicate MCM-41 samples were prepared with increasing amounts of aluminum isopropoxide in the synthesis gel, treated as described above, and then analyzed for bulk aluminum concentrations in the as-synthesized and calcined products using elemental analyses. For syntheses in which the molar Si/Al ratios in the gels were greater than one (MCM-41a,b), higher concentrations of aluminum in the synthesis gels produced higher aluminum concentrations in the bulk MCM-41 products (Table 1). Moreover, the solid products in each case possessed higher Al contents than the respective starting gels. This indicates preferential uptake of hydrolyzed aluminum species from the alkoxide precursor solutions, compared to the silica species also available. For example, MCM-41a with a molar Si/Al ratio of 8.0 in the synthesis gel was observed to have Si/Al ratios of 4.6 and 5.0 in the as-synthesized and calcined products, respectively. MCM-41b also had significantly lower bulk Si/Al ratios for the as-synthesized and calcined products (Si/Al = 2.9), in comparison to the synthesis gel composition (Si/Al = 4.0). Under these alkaline reaction conditions, beginning with partially hydrolyzed $Al(O^iPr)_3$ and initially non-hydrolyzed TEOS favors aluminum incorporation into the polymerizing aluminosilicate framework. Silica monomers from TEOS that are not included in the mesophase framework remain in the aqueous synthesis solution and are washed away upon filtration.

Syntheses in which the molar Si/Al ratios in the gels were equal to or less than one (MCM-41c,d) show final products in which the bulk Si/Al ratios approach an apparent limiting value of unity for both as-synthesized and calcined materials (Table 1). This indicates that for the MCM-41 synthesis conditions examined here, Lowenstein's rule excluding Al−O−Al linkages in the framework is apparently obeyed: hydrolyzed aluminum species tend to copolymerize with silica monomers in a close to alternating fashion within the aluminosilicate network. It should be noted that an entirely alumina mesoporous framework, composed predominantly of octahedrally coordinated aluminum, can be synthesized by using anionic surfactants with carboxylate head groups, although the resulting product lacked a high degree of mesostructural ordering.[25]

Elemental analyses provide composition information that is averaged over bulk (milligram) quantities of sample, irrespective of material heterogeneities. Thus, it is not possible to distinguish between aluminum species that have been incorporated into an M41S framework and different nonframework aluminum species that may be present as undesirable byproducts within a bulk sample. The possibility exists that Si and Al species are partitioned heterogeneously among different macroscopic domains. For this reason, the bulk Si/Al molar ratios in the final product should be regarded cautiously. Other methods, in particular solid-state 2D NMR, must be relied on to establish the framework locations of aluminum species present[23] and thereby justify the claim that low silica materials are being produced from the synthesis methods outlined.

3.2. X-ray Powder Diffraction. Mesoscopic ordering of the as-synthesized and calcined low silica M41S products was characterized using X-ray powder diffraction, which also permitted the structural stabilities of

(24) Earl, W. L. Personal communication.

(25) Vaudry, F.; Khodabandeh, S.; Davis, M. E. *Chem. Mater.* **1996**, *8*, 1451−1464.

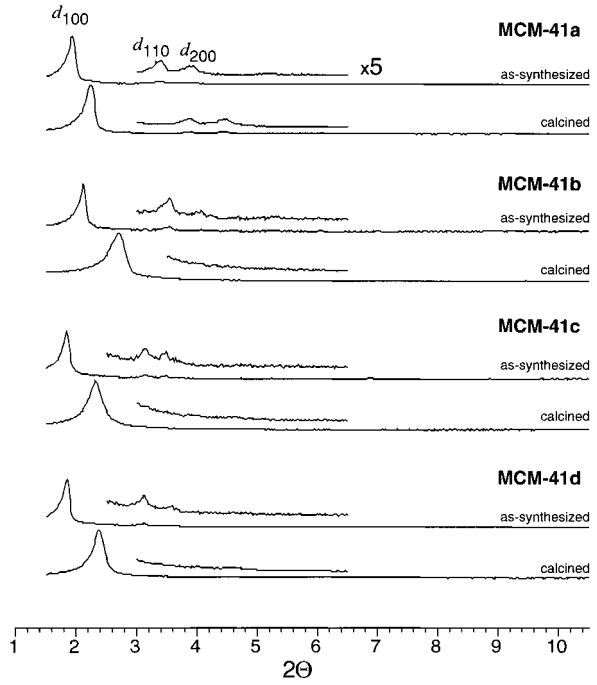

Figure 1. X-ray powder diffraction patterns for low silica MCM-41 materials (see Table 1) prepared at room-temperature with molar Si/Al gel ratios of 0.5 (bottom), 1.0, 4.0, and 8.0 (top). Prior to calcination, d_{100}, d_{110}, and d_{200} reflections are present for all of the materials. After calcination, diminished intensities of the d_{110} and d_{200} reflections are observed and the d_{100} spacings decrease by up to 20% for the samples with the higher aluminum contents.

the materials to be examined. Reaction mixtures using CTAB as the structure-directing surfactant species under the conditions described above, resulted in the formation of hexagonally ordered aluminosilicate MCM-41 materials, as evidenced by the well-resolved (100), (110), and (200) scattering reflections shown in Figure 1. The XRD patterns for the as-synthesized samples are typical of MCM-41 materials made using this cationic surfactant with 16-carbon atoms in its hydrophobic alkyl chain. For example, d_{100}, d_{110}, and d_{200} peaks are observed at 46.5, 26.9, and 22.4 Å, respectively, for the as-synthesized aluminosilicate MCM-41a product. Despite the high aluminum contents of this and the other samples, the structures for the as-synthesized materials retain the long-range mesoscopic ordering of hexagonal *p*6*mm* phases, characteristic of high-quality MCM-41 materials.

Calcination of the as-synthesized MCM-41 materials removes the surfactant species to produce mesoporous aluminosilicate solids, whose XRD patterns are shown in Figure 1 below those for each of the as-synthesized samples. For the MCM-41a sample, which contained a relatively low amount of aluminum in the reaction gel and in the final product, all of the reflections measured for the as-synthesized material are retained following calcination, albeit with an approximately 10% reduction in the lattice parameters. For the MCM-41 materials prepared using synthesis gels with Si/Al molar ratios less than 4.0, the relative intensities of the higher angle reflections are diminished significantly with respect to the d_{100} reflections, which additionally decrease by approximately 20%. The decreased intensities of the higher angle XRD reflections indicate reduced mesoscopic order in the samples. Together with the large contractions of the lattices measured following calcination (see *d* spacings, Table 1), these observations confirm that the low silica MCM-41 materials are less thermally stable and less structurally robust than their more siliceous analogs. Similar results have been found for zeolitic materials, where increased aluminum contents in silicate frameworks provide greater reactivity, though at the cost of lower thermal stability.[14] Nevertheless, the decreased mesoscopic organization is not accompanied by the appearance of significant scattering intensity from amorphous byproducts of the calcination procedure. Thus, while the long-range hexagonal order of the low silica MCM-41 systems are reduced by the calcination treatments, they do not appear to be accompanied by the general collapse of large portions of the mesoscopic structures.

3.3. Solid-State NMR. *As-Synthesized Low Silica MCM-41.* At a molecular level, one-dimensional (1D) ^{27}Al and ^{29}Si MAS NMR spectra can be used to establish the coordination and degree of local order of aluminum and silicon atoms in the MCM-41 samples. Figure 2 contains a series of 1D ^{27}Al and ^{29}Si MAS spectra acquired for the as-synthesized materials prepared with different concentrations of aluminum in the synthesis gels. All of the ^{27}Al MAS spectra in Figure 2a contain a single peak centered at 55 ppm (1.3 kHz fwhm), which can be assigned to tetrahedrally-coordinated ^{27}Al atoms that are bonded to next-nearest-neighbor silicon atoms via bridging oxygen atoms in the aluminosilicate network.[13] Weak spinning sidebands appear symmetrically on either side of the main ^{27}Al peaks. Despite the high concentrations of aluminum present in these syntheses, little if any spectral intensity (besides the small spinning sidebands) is observed in the regions of 30 ppm or 0 ppm, where signals corresponding to aluminum atoms in five- or six-coordinate environments, respectively, are typically observed.[13]

The corresponding ^{29}Si MAS spectrum for each as-synthesized low silica MCM-41 sample is shown alongside its respective ^{27}Al MAS spectrum in Figure 2b. For these materials, peaks or shoulders in the ^{29}Si MAS spectra arise from silicon atoms in fully or partially polymerized sites with different numbers of silicon next-nearest neighbors. For such silicon species in aluminosilicate materials, different sites can be classified using the notation $Q^n(m\ \mathrm{Al})$, which denotes a central silicon atom bound via bridging oxygen atoms to *n* next-nearest neighbor silicon and aluminum atoms, *m* of which are Al.[13] Progressing from top to bottom in Figure 2b, it is clear that as the concentration of aluminum isopropoxide is increased in the synthesis gel, the relative number of Si−O−Al linkages increases at the expense of fewer Si−O−Si moieties. This is manifested by the increased downfield signal intensities observed in the ^{29}Si MAS spectra for samples MCM-41c,d compared to broader upfield signals observed for samples MCM-41a,b. For the low silica MCM-41c,d materials with bulk molar Si/Al ratios of 1.3, the ^{29}Si MAS spectra show relatively narrow signals at −85 ppm arising predominantly from fully polymerized Q^4(4 Al) ^{29}Si species.[26] In contrast, significantly broader linewidths are observed upfield in the ^{29}Si MAS spectra of samples MCM-41a,b, for which bulk Si/Al ratios of 4.6 and 2.9 have been

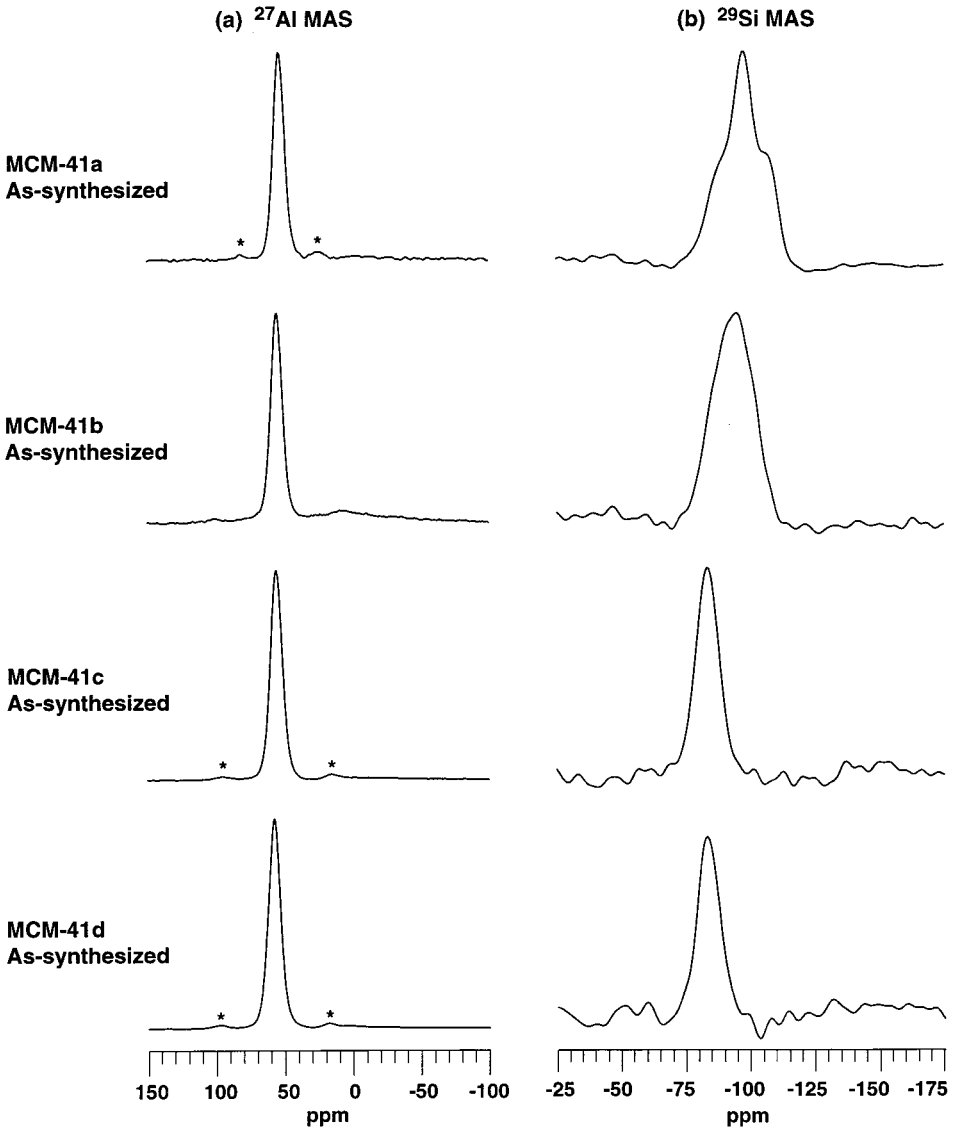

Figure 2. Single-phase ^{27}Al and ^{29}Si MAS NMR spectra for as-synthesized, low silica MCM-41a−d samples containing different concentrations of aluminum (see Table 1). (a) Only tetrahedrally coordinated aluminum species (55 ppm) are observed in the ^{27}Al MAS spectra of these materials. The additional weak peaks in the spectra correspond to spinning sidebands (∗) which appear symmetrically about the isotropic peak at integer multiples of the rotor frequency. ^{27}Al MAS data were collected with short 1-μs pulses (corresponding to a $\pi/6$ tip angle), 500-ms repetition delays, and spinning speeds ranging from 3.5 to 5 kHz under conditions of proton decoupling. (b) ^{29}Si MAS spectra reflect a distribution of ^{29}Si sites. ^{29}Si MAS data were collected with a 8.50-μs $\pi/2$ pulse and a recycle delay of 180 s, under conditions of magic-angle spinning at 5 kHz and proton decoupling.

measured, respectively. For these samples, the ^{29}Si atoms in fully polymerized Q^4 and partially polymerized Q^3 sites will have a lower probability of having Al next-nearest neighbors, as confirmed by signals with chemical shifts in the range −90 to −110 ppm.[26]

Whereas crystalline aluminosilicate zeolites generally possess frameworks in which aluminum (and silicon) sites are tetrahedrally coordinated, establishing whether four-coordinate aluminum species are necessarily incorporated into the amorphous frameworks of aluminosilicate M41S materials is difficult and less certain. The appearance of four-coordinate Al species in amorphous alumina phases, for example, has been observed in aluminosilicate and sol−gel derived glasses.[27] Furthermore, it has been shown that phase-separated amorphous byproducts containing exclusively four-coordinate aluminum species can result from M41S syntheses.[9] It is generally not possible to resolve such issues on the basis of 1D ^{27}Al and ^{29}Si MAS results alone. However, two-dimensional solid-state NMR methods can be used to obtain additional insights into the molecular structures of M41S materials from which more precise structural conclusions can be made regarding the location and chemical nature of the aluminum species.[23]

(26) The existence of Q^4(3 Al) silica species in samples MCM-41c and MCM-41d cannot be entirely ruled out; however, the symmetric ^{29}Si MAS peaks centered about the range typical of Q^4(4 Al) species suggests that the fraction of Q^4(3 Al) species is small. Similarly in samples MCM-41a and MCM-41b, incompletely polymerized Q^2 and Q^3 silica species, including those with silanol groups, may be present and contribute some signal intensity to the ^{29}Si MAS spectra in the region −90 to −100 ppm.

(27) Engelhardt, G.; Nofz, M.; Forkel, K.; Wihsmann, F. G.; Mägi, M.; Samoson, A.; Lippmaa, E. *Phys. Chem. Glasses* **1985**, *26*, 157−165. Cho, I. H.; Park, S. B.; Kwak, J. H. *J. Mol. Catal. A* **1996**, *104*, 285−291. Gerardin, C.; Sundaresan, S.; Benziger, J.; Navrotsky, A. *Chem. Mater.* **1994**, *6*, 160−170.

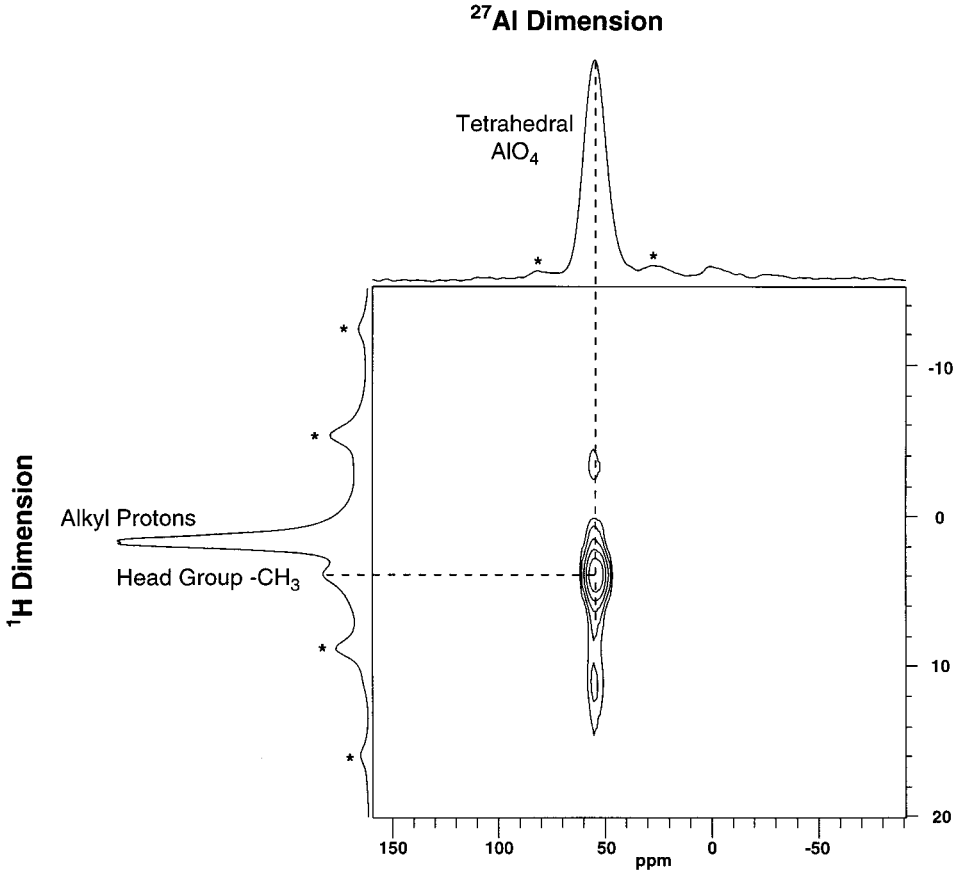

Figure 3. Two-dimensional ^{27}Al{^{1}H} HETCOR NMR spectrum for as-synthesized, low silica MCM-41d (Si/Al = 1.3). Separate ^{27}Al MAS and ^{1}H MAS spectra accompany the HETCOR contour plot along the corresponding axes (* denotes spinning sidebands). The 2D spectrum was acquired at room-temperature under conditions of magic-angle spinning at 3.5 kHz. A 8.0-μs 90° pulse, followed by a 0.75-ms contact time, was used for cross-polarization. The 90° ^{27}Al pulse length was assumed to be one-third of the 90° pulse length found for ^{27}Al in solution.[28,29] The HETCOR intensity correlations spectrum show that the tetrahedrally coordinated aluminum species interact strongly with the protons of the surfactant head group.

Here, we use two-dimensional (2D) *het*eronuclear chemical shift *cor*relation (HETCOR) NMR spectroscopy to correlate ^{1}H and ^{27}Al resonances and thereby identify aluminum species that interact strongly with specific protonated moieties. In particular, such moieties may be the trimethylammonium head groups of the structure-directing CTA^+ surfactant molecules, the alkyl surfactant tails, or adsorbed water. For Al species that are tetrahedrally coordinated to bridging oxygen atoms in aluminosilicate MCM-41 frameworks of the as-synthesized materials, accompanying anionic charges lead to strong interactions between these aluminum sites and the cationic head-groups of the surfactant species. As a consequence of this, strong heteronuclear dipole-dipole couplings exist between framework ^{27}Al nuclei and protons of the trimethylammonium head-group moieties.[23]

A 2D ^{27}Al{^{1}H} HETCOR spectrum is shown in Figure 3 for the as-synthesized MCM-41d sample (Si/Al = 1.3). The ^{27}Al{^{1}H} designation denotes that, for this HETCOR experiment, magnetization produced by excitation of the ^{1}H nuclei was transferred to nearby ^{27}Al nuclei, which were subsequently detected. Separately acquired 1D ^{27}Al{^{1}H} cross-polarization (CP) MAS and ^{1}H MAS spectra are plotted along the horizontal and vertical axes, respectively, of Figure 3 to aid the interpretation of the 2D spectrum, which is presented as a contour plot. In the 2D ^{27}Al{^{1}H} HETCOR contour spectrum, strong peak intensity is observed at a position in the 2D frequency map that demonstrates a clear correlation between resonances from tetrahedrally coordinated aluminum species (55 ppm) and protons associated with the CTA^+ head groups (3.4 ppm). Above and below the main peak in the ^{1}H dimension of the 2D data set are spinning sidebands, which occur at integer multiples of the MAS rotor frequency and arise here from the $-CH_3$ moieties of the surfactant head groups. No significant correlated intensity is observed from coupling between the tetrahedral ^{27}Al species and protons from the alkyl tails of the surfactant molecules for the short 0.75-ms ^{1}H$-^{27}$Al contact time used. Compared to the CTA^+ head groups, the alkyl chain moieties are more mobile and spatially more distant from the aluminosilicate framework interface, resulting in reduced efficiency of ^{1}H$-^{27}$Al dipole$-$dipole couplings between these species. Thus, the ^{27}Al{^{1}H} HETCOR spectrum establishes conclusively that a significant fraction of the tetrahedrally coordinated aluminum species are in molecular proximity to the head groups of the structure-directing surfactant molecules. These results, in conjunction with XRD and elemental analysis measurements, confirm the incorporation of tetrahedrally coordinated aluminum atoms into the aluminosilicate frameworks of the as-synthesized MCM-41d material, which approaches Lowenstein's limit of Si/Al = 1.

Calcined Low Silica MCM-41. Solid-state ^{27}Al and ^{29}Si MAS NMR studies performed on calcined mesoporous aluminosilicate MCM-41 samples provide insight

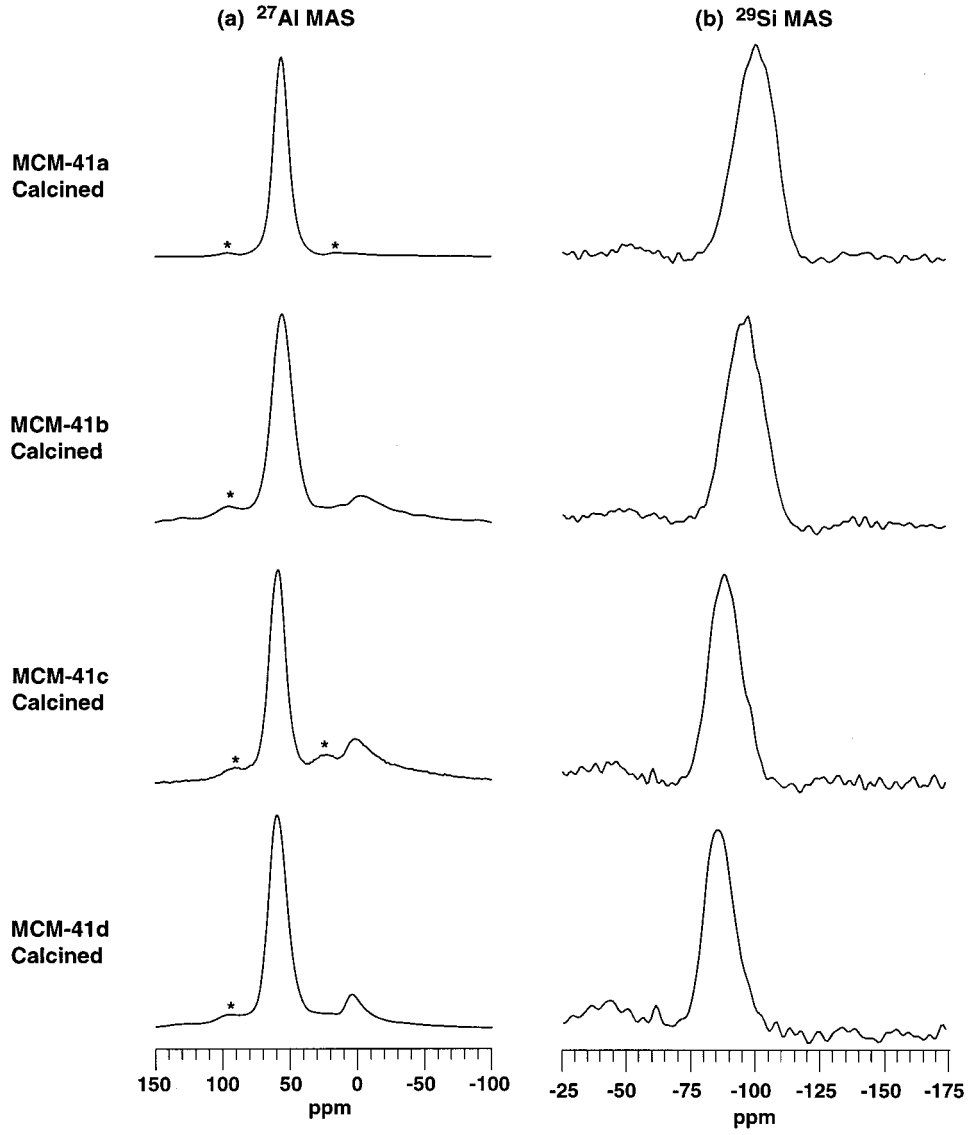

Figure 4. Single-pulse ^{27}Al and ^{29}Si MAS NMR spectra for low silica MCM-41a−d samples after calcination. (a) The ^{27}Al MAS spectra each contain a dominant ^{27}Al peak at 55 ppm corresponding to tetrahedrally coordinated aluminum and a minor feature at 0 ppm corresponding to octahedrally coordinated aluminum. (b) The ^{29}Si MAS spectra show peaks with increased line widths compared to the as-synthesized materials (Figure 2b), indicating broader distributions of ^{29}Si environments in the calcined samples. The ^{27}Al and ^{29}Si data were collected using the experimental conditions as reported in Figure 2.

into the molecular-level changes that have occurred in these materials following high-temperature treatment to remove the surfactant species. As shown in Figure 1 and discussed above, XRD patterns for each of the calcined materials indicate that long-range mesoscopic order is retained, though to a reduced extent at higher Al concentrations. The dominant peak at 55 ppm in the ^{27}Al MAS spectra of Figure 4a indicates that four-coordinate aluminum species remain a large component fraction in each of the calcined MCM-41 samples. A minor octahedrally-coordinated aluminum component is also present, as evidenced by the small peak near 0 ppm in each of the spectra. Weak intensity from spinning sidebands (∗) can be detected symmetrically about the ^{27}Al peak associated with the four-coordinate aluminum sites.

The 2D ^{27}Al{^{1}H} HETCOR spectrum in Figure 5 confirms that a substantial fraction of the tetrahedrally coordinated aluminum species in the calcined material remains incorporated in the calcined low silica MCM-41d framework (bulk Si/Al = 1.0). Following calcination of the MCM-41d sample and subsequent ion-exchange with NH_4^+, the 2D ^{27}Al{^{1}H} HETCOR spectrum reveals a strong intensity correlation between signals from tetrahedrally coordinated aluminum species and protons associated with the exchangeable ammonium cations. Little or no correlated intensity appears to exist between the protons associated with the silanol groups and the aluminum atoms in the framework, indicating that these moieties do not interact strongly and may not be molecularly proximate to one another. Similar results have been obtained for the calcined MCM-41a material containing lower concentrations of aluminum.[23] These results demonstrate the accessibility of tetrahedral Al species to exchangeable cations and confirm directly the presence of four-coordinate aluminum in the low silica MCM-41 frameworks after calcination.

In comparing the 1D ^{27}Al MAS NMR spectra for the as-synthesized and calcined materials in Figure 2a and 4a, respectively, one observes some degree of broadening of the ^{27}Al peaks for the calcined samples, though otherwise the spectral features are similar. This is

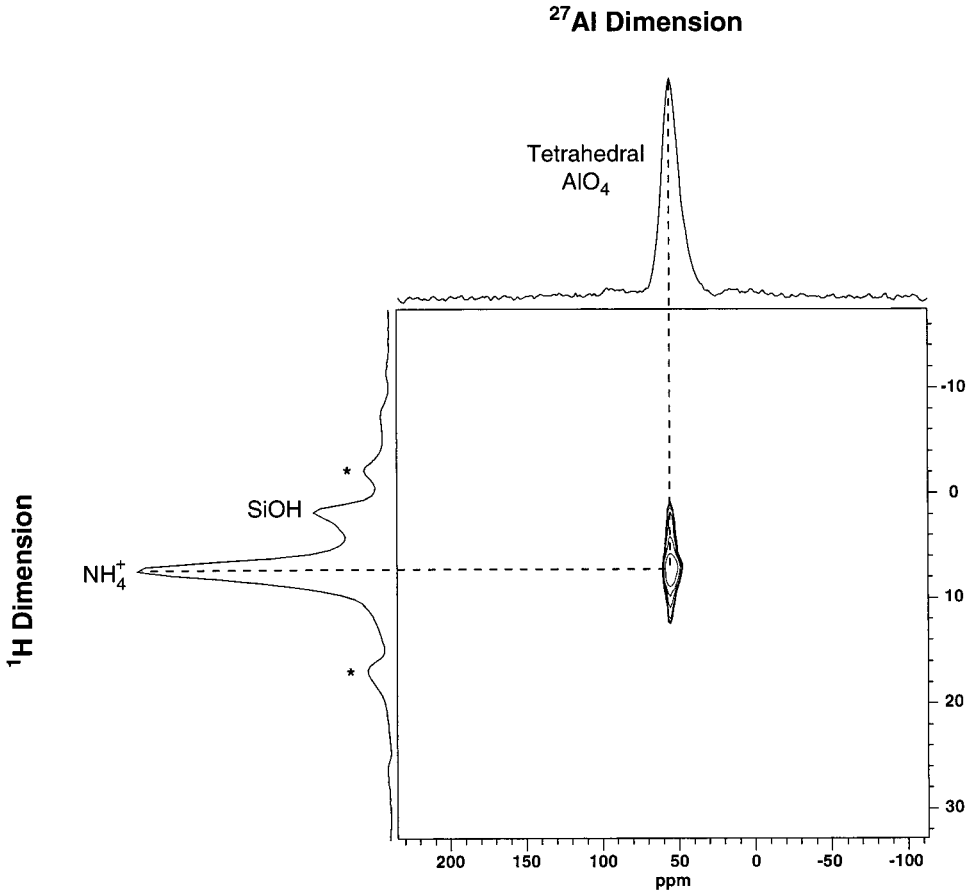

Figure 5. Two-dimensional ^{27}Al{^{1}H} HETCOR spectrum for the calcined, NH_4^+-exchanged, and dehydrated aluminosilicate MCM-41d sample. Separate ^{27}Al MAS and ^{1}H MAS spectra accompany the HETCOR contour plot along the corresponding axes. Correlated intensity in the 2D spectrum between signals from the NH_4^+ protons and tetrahedrally coordinated ^{27}Al species confirm retention of aluminum atoms in the framework following calcination. The spectra were acquired using the same experimental conditions reported in Figure 3.

despite a relatively sharp decrease in the ^{27}Al signal intensities observed in the MAS spectra of the calcined materials, which required several thousand acquisitions to achieve acceptable signal-to-noise levels. In comparison, several hundred acquisitions were sufficient for the as-synthesized materials. For the calcination conditions used, no volatility of aluminum species is expected. However, the net loss of ^{27}Al signal intensity observed following calcination of the as-synthesized materials indicates that partial dealumination of the aluminosilicate framework apparently has occurred. This is supported by ^{29}Si MAS spectra in Figure 4b from each of the calcined MCM-41 samples, which show broader and less well resolved ^{29}Si MAS peaks than for the as-synthesized materials (Figure 2b). In each case, the broader ^{29}Si peaks are also shifted upfield, indicating that the silicon atoms possess on average fewer Al next-nearest neighbors after calcination. The larger frequency ranges spanned by the ^{29}Si signals reflect distributions of silica species with different numbers of next-nearest-neighbor silicon atoms (from zero to four, accordingly), which are produced as a result of partial dealumination of the MCM-41 frameworks during calcination treatment.

In the absence of ^{27}Al NMR signals, XRD reflections, or other measurements to account directly for products of the dealumination process, the loss of intensity in the ^{27}Al MAS spectra of Figure 4a apparently reflects the transformation of tetrahedrally coordinated framework aluminum sites into so-called "NMR invisible" ^{27}Al species. This has been a challenging issue in zeolite catalysis, due to the difficulty of characterizing aluminum species in highly disordered asymmetric environments.[30] However, by using an internal standard (*e.g.*, AlN) of known mass to calibrate the ^{27}Al MAS spectra, the decrease in ^{27}Al signal intensity can be monitored quantitatively to estimate the fraction of aluminum to which this label may apply. For example, Figure 6 shows calibrated ^{27}Al MAS spectra acquired under identical conditions and for identical precalcined quantities of the MCM-41a material before (Figure 2a) and after calcination (Figure 4a). Both ^{27}Al MAS spectra in Figure 6 have been normalized to the intensity of the isotropic signal at 113 ppm from the same AlN standard, which permits the intensities of the other ^{27}Al peaks in the superimposed spectra to be compared. In particular, the peak at 55 ppm attributed to tetrahedrally coordinated aluminum species is of primary interest. Other features present in the spectra include numerous spinning sidebands associated with the AlN peak that occur at integer multiples of the rotor spinning frequency offset from the centerband; the weak signal near 10 ppm

(28) Schmidt, V. H. *Pulsed Magn. Opt. Reson., Proc. Ampère Int. Summer School*, **1971**, *2nd*, 75−83.
(29) Fenzke, D.; Freude, D.; Fröhlich, T.; Haase, J. *Chem. Phys. Lett.* **1984**, *111*, 171−175.
(30) Vega, A. J.; Luz, Z. *J. Phys. Chem.* **1987**, *91*, 365−373. Luz, Z.; Vega, A. J. *J. Phys. Chem.* **1987**, *91*, 374−382.

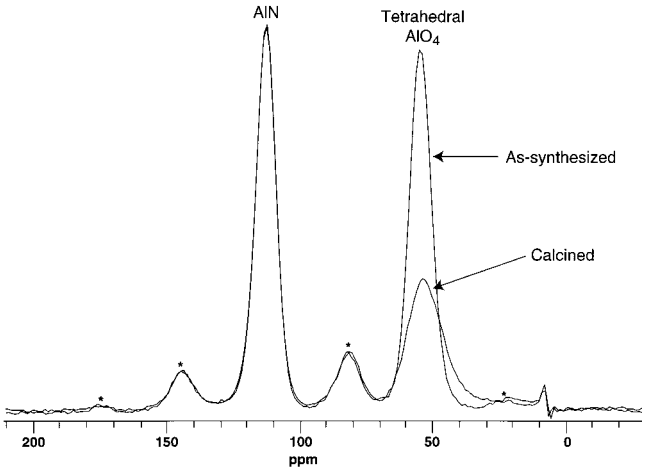

Figure 6. Al MAS NMR spectra for as-synthesized and calcined low silica MCM-41a acquired using aluminum nitride as an internal standard to calibrate the detectable ^{27}Al signals. The data were collected using an identical number of acquisitions and experimental conditions as reported in Figure 2, except a recycle delay of 60 s was used to accommodate the longer T_1 relaxation time of AlN. Superimposed spectra are shown for identical amounts of sample (measured before calcination) and identical acquisition and processing parameters. Compared to the as-synthesized samples, the calcined material shows diminished signal intensity at 55 ppm relative to the AlN peak at 113 ppm which indicates a decrease in the number of tetrahedrally coordinated aluminum species. Deconvolution of these spectra indicate an approximately 50% loss of signal from tetrahedral aluminum species following calcination without a significant appearance of additional six-coordinate aluminum species.

Table 2. Percent Reductions in the Integrated Areas of the ^{27}Al MAS NMR Peaks Associated with Tetrahedrally Coordinated Aluminum Following Calcination of the Low Silica MCM-41 Materials (See Figure 6)

sample	^{27}Al MAS signal reduction (%)
MCM-41a	50 ± 5
MCM-41b	55 ± 5
MCM-41c	53 ± 5
MCM-41d	48 ± 5

corresponds to a small amount of octahedrally coordinated aluminum impurity in the AlN standard.

Calibration of the ^{27}Al MAS spectra in this way allows the relative intensities of the tetrahedrally coordinated Al peaks to be measured and compared for the as-synthesized and calcined samples and the relative number of ^{27}Al spins in each to be established. Accordingly, the integrated ^{27}Al signal from tetrahedrally coordinated species is diminished by approximately 50% following calcination of the as-synthesized MCM-41a material. This is in spite of the fact that independent elemental analysis shows that the bulk aluminum concentration in the sample remains unchanged (within the uncertainty of the measurements) after calcination treatments. Similar results were observed for each of the other low silica MCM-41 materials, as shown in Table 2. No corresponding increases in the signals associated with octahedrally coordinated aluminum are observed to compensate for the decreased peak intensities from the four-coordinate Al species. Consequently, we speculate that excessive ^{27}Al line-broadening, due to large and/or broad distributions of second-order quadrupolar coupling parameters, accounts for the disappearance of a significant fraction of the aluminum

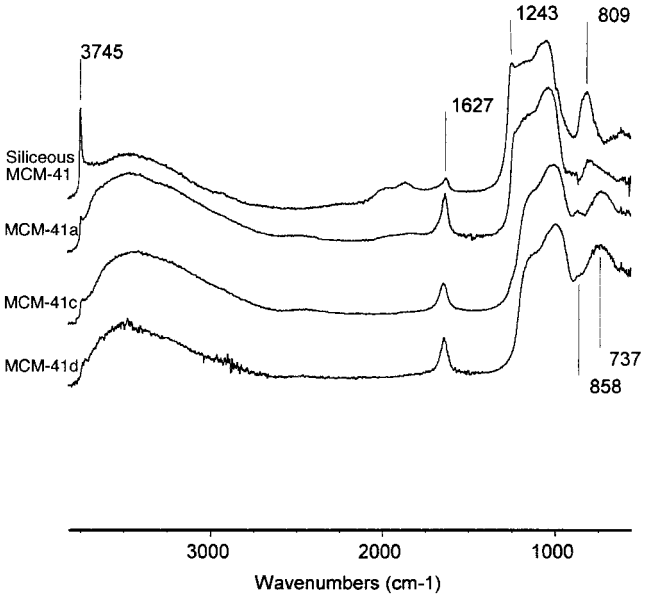

Figure 7. Photoacoustic infrared spectra for a series of calcined MCM-41 materials prepared from synthesis gels with molar Si/Al ratios of ∞ (siliceous), 8.0, 1.0 and 0.5, the latter three corresponding to samples MCM-41a,c,d, respectively. As the aluminum content is increased, the IR spectra show substantially reduced intensities at 3745 cm^{-1} from Si−OH moieties and shifts in the bending vibrations near 800 and 1000−1200 cm^{-1} to lower wavenumbers.

signal. The existence, structures, and catalytic significance of such "NMR invisible" aluminum species associated with zeolite activation have been actively pursued for many years using specialized techniques for their characterization.[30−33]

3.4. Infrared and BET Characterization. Corroborative evidence for the incorporation of aluminum into the low silica MCM-41 frameworks of the calcined materials is provided by photoacoustic infrared (IR) spectra in Figure 7. With increased aluminum contents of the bulk samples, changes are observed in the photoacoustic IR spectra that reflect increased aluminum concentrations in the aluminosilicate frameworks. In particular, the IR spectra show evidence of Al−O−Si bending vibrations in the vicinity of 800 and 1000−1200 cm^{-1}, which appear at lower wavenumbers as the aluminum contents of the frameworks increase. In addition, aluminum incorporation into the MCM-41 frameworks causes an abrupt decrease in the intensity of the silanol peak at 3745 cm^{-1}, which is barely visible in the spectra for calcined samples MCM-41a,c,d. This observation is consistent with recent 2D ^{27}Al{^{1}H} HETCOR measurements of MCM-41a,[23] which show that silanol groups appear to be distant from four-coordinate Al sites and may decrease in number with increasing aluminum content of the framework. The loss of overtone frequencies in the range 1700−2200 cm^{-1} remains under investigation.

Sorption analyses of the calcined low silica MCM-41 materials support observations that increased alumi-

(31) Grey, C. P.; Vega, A. J. *J. Am. Chem. Soc.* **1995**, *117*, 8232−8242.
(32) Ernst, H.; Freude, D.; Wolf, I. *Chem. Phys. Lett.* **1993**, *212*, 588−596. Freude, D.; Ernst, H.; Wolf, I. *Solid State Nucl. Magn. Reson.* **1994**, *3*, 271−286.
(33) Hunger, M.; Horvath, T.; Engelhardt, G.; Karge, H. G. *Stud. Surf. Sci. Catal.* **1995**, *94*, 756−763. Hunger, M.; Horvath, T. *Ber. Bunsen-Ges. Phys. Chem.* **1995**, *99*, 1316−1320.

Table 3. BET Surface Areas and Mean Pore Sizes for Calcined Low Silica Aluminosilicate MCM-41 Materials, As Determined from Nitrogen Adsorption Isotherm Measurements

sample	BET surface area (m^2/g)	mean pore size (±2 Å)
MCM-41a	1031 ± 8	29
MCM-41b	660 ± 7	22
MCM-41c	603 ± 3	19
MCM-41d	396 ± 14	26

num concentrations in the frameworks result in greater contraction or, in the extreme, partial collapse of the mesostructures during calcination. Table 3 reports the average surface areas and pore sizes determined from BET analyses of the nitrogen adsorption isotherms for the calcined low silica mesoporous MCM-41 materials. With increasing aluminum content, the average BET surface area of the respective calcined samples decreases from 1031 m^2/g for MCM-41a to 603 m^2/g for MCM-41c. The average BET pore sizes in these materials also tend toward smaller dimensions with increasing aluminum concentration. Analysis indicates that the pore size for the MCM-41d material, which was prepared in the presence of excess aluminum, appears to contain a contribution from large macropores, possibly arising from alumina species that are not incorporated into the MCM-41d framework or regions where local framework collapse has occurred. The BJH method, which was used to calculate pore size distributions from nitrogen adsorption data independently of the BET isotherm model, shows a maximum number of pores in the MCM-41d sample with average diameters of 20.6 Å. This value is consistent with the trends observed for the aluminum contents of the samples (see Table 1), though it is near the size limit of the BJH analysis.

Conclusions

Low silica aluminosilicate MCM-41 materials have been prepared with high concentrations of aluminum in tetrahedral framework sites with bulk molar Si/Al ratios approaching unity while retaining long-range mesoscopic order. ^{27}Al and ^{29}Si NMR techniques, in conjunction with XRD and photoacoustic IR, provide a self-consistent body of evidence for the preparation of mesoscopically ordered low silica framework structures. In particular, two-dimensional $^{27}Al\{^{1}H\}$ heteronuclear chemical shift correlation NMR experiments verify aluminum incorporation in the frameworks of as-synthesized and calcined low silica MCM-41 materials. As more aluminum was incorporated, the thermal stabilities of the materials decreased. Following calcination, reduced intensities in higher angle reflections of the XRD patterns and ^{27}Al and ^{29}Si MAS NMR data reveal decreased mesoscopic and molecular order, providing evidence for partial dealumination of the framework that has been estimated quantitatively. The results here represent the highest reported aluminum contents for well-ordered aluminosilicate M41S materials, for which the incorporation of four-coordinate aluminum species into the inorganic oxide frameworks has been confirmed. Similar synthesis strategies have permitted mesoporous aluminosilicate MCM-48, with a highly ordered cubic mesostructure, to be prepared with a bulk molar Si/Al ratio of 8.[34] Such materials are expected to possess increased capacities for adsorption and ion exchange, as well as the potential for improved catalytic activities. Such applications, however, may be limited by the relatively low hydrothermal stabilities of these materials. Efforts aimed at improving their robustness are currently underway in our laboratories.

Acknowledgment. We thank Dr. F. Babonneau and Prof. J. P. Jolivet for helpful discussions. This work was supported by the NSF Young Investigator Program (B.F.C.), Shell Research B.V. (B.F.C.), and NSF Grant DMR-9520971 (G.D.S.). The experiments were conducted on NMR instrumentation supported in part by the NSF Division of Materials Research under Grant DMR-9222527 and through the UCSB Materials Research Laboratory under Award DMR-9632716. M.T.J. acknowledges partial support from the Biotechnology Research and Education Program of the University of California. S.C.C. is supported by funding from the U.S. Army Research Office under grant DAAH04-96-1-0443. B.F.C. is a Camille and Henry Dreyfus Teacher−Scholar and an Alfred P. Sloan Research Fellow.

CM981135V

(34) Janicke, M. T., Ph.D. dissertation, Dept. of Chemical Engineering, University of California at Santa Barbara, 1997.